MEDWIN PUBLISHERS
Committed to Create Value for Researchers

International Journal of Biochemistry & Physiology
ISSN: 2577-4360

An Efficient and Affordable Method for Isolating Bone Marrow-Derived Mesenchymal Stem Cells from Swiss Albino Mice

Chauhan A and Kumar Gautam P*

All India Institute of Medical Sciences (AIIMS), India

***Corresponding author:** Pramod Kumar Gautam, Additional Professor, Department of Biochemistry, All India Institute of Medical Sciences (AIIMS), New Delhi, India, Tel: 9838442087 & 01126594682; Emails: gautam@aiims.edu / pamodgautam_13@yahoo.com

Research Article

Volume 11 Issue 1

Received Date: May 19, 2026

Published Date: June 29, 2026

DOI: 10.23880/ijbp-16000271

Abstract

Introduction: There are several ways to isolate MSCs, such as using immunomagnetic kits. However, these approaches are costly and not always suitable for large-scale or frequent animal studies. This study aimed to provide a cost-effective, reproducible protocol, purification, and functional characterization of BM-MSCsresearch.

Materials and Methods: Swiss albino mice (8-12 weeks, 20-25 g) were housed in pathogen-free conditions in accordance with IAEC rules. We used morphological evaluation, fluorescence microscopy, and flow cytometry to look at BM-MSCs and find MSC markers (CD44, CD90, and CD105) and negative markers (CD45 and CD31). Quantitative real-time PCR was used to look at the gene expression of epithelial-mesenchymal transition (EMT) and tumor-associated markers (N-cadherin, Nectin, Notch).

Results: BM-MSCs were successfully isolated, initially exhibiting a rounded morphology that progressively transitioned into a spindle-shaped fibroblastic configuration by days 3 to 5, reaching 60 to 70% confluence by day 7. ICC of P-3 BM-MSCs demonstrated strong expression of mesenchymal markers CD44 and CD90. Flow cytometry analysis revealed a progressive enrichment of MSCs over passages, with $CD44^+/CD105^+$ cells increasing from 0.059% at P-1 to 71.9% at P-2 and ultimately reaching 92.0% at P-3, while remaining negative for CD31 and CD45.

Conclusion: This study establishes a comprehensive, reproducible protocol for isolating and characterizing MSCs and generating tumor-conditioned MSCs and validating phenotypic. The improved method provides a substantial foundation for investigating MSC-tumor interactions and developing MSC-based therapeutic strategies.

Keywords: Bone Marrow Mesenchymal Stem Cells; Tumor-Conditioned Mscs; EMT Markers; Flow Cytometry; Immunocytochemistry; Breast Cancer

Abbreviations

MSCs: Mesenchymal Stem Cells, TC: Tumor-Conditioned; EMT: Epithelial-Mesenchymal Transition; ER; Estrogen Receptor; FBS: Fetal Bovine Serum; SE: Standard Error; BM-MSCs: Bone Marrow-Derived Mesenchymal Stem Cells; ICC: Immunocytochemistry.

Introduction

Mesenchymal stem cells (MSCs) are multipotent stromal cells capable of developing into several cell types, including

osteoblasts, adipocytes, and chondrocytes, and possess immunomodulatory properties. It facilitates the sustenance of other cells and participates in epithelial-mesenchymal transition. It may facilitate tumor growth by engaging with tumor cells via paracrine signaling and differentiating into various cell types [1-3]. MSCs actively influence cancer cells via many methods, including the CXCL1/CXCL5-chemokine (C-X-C motif) receptor 2 (CXCR2), CCL5, IL-6, estrogen receptor (ER), and CXCR4 pathways in breast cancer. MSCs promote the invasive and metastatic potential of tumor cells via the secretion of CCL5 [4-7]. It is well-established that both human and murine MSCs play a significant role in metastasis across many cancer types. In tumor stroma, MSCs have been shown to migrate and develop into cancer-associated fibroblasts (CAFs), hence facilitating tumor growth. At the primary tumor site, MSCs stimulate angiogenesis by releasing many soluble factors, including M-CSF, leukemia inhibitory factor, MIP-2, VEGF, TNF-α, and IFN-γ. SC establishes a cancer stem cell niche, facilitating carcinogenesis by the synthesis of substantial quantities of prostaglandin E2 [4-10]. A wide array of cytokines released by MSCs, including TGF-β, IL-10, nitric oxide, prostaglandin E2, and indoleamine 2,3-dioxygenase, is involved in immunomodulation [11-15]. The utilization of MSCs in diverse applications, including immunomodulation, tumor growth, and other pathophysiological situations, presents many prospects for future advancement [16,17].

This work sought to provide a cost-efficient, repeatable, and optimal technique for the separation, purification, and functional characterization of bone marrow-derived mesenchymal stem cells (BM-MSCs) and their tumor-induced transformation. This work included the isolation of BM-MSCs from the tibia and femur of Swiss albino mice by a plastic adherence approach, followed by characterization via morphology, immunocytochemistry, and flow cytometry. The separated cells exhibited a characteristic spindle morphology. They exhibited MSC-specific markers including CD44, CD90, and CD105. Nonetheless, they lacked hematological or endothelial markers such as CD45 and CD31. This resembled MSCs derived from commercial kit methodologies. Tumor conditioning originated with the use of conditioned media derived from the C127I breast cancer cell line. The procedure resulted in enhanced cellular proliferation and significant alterations in cellular attributes. Significantly, tumor-conditioned MSCs exhibited an increase in markers associated with epithelial-mesenchymal transition, such as N-cadherin, Nectin, and Notch. This indicates a change in function. This enhanced methodology offers a cost-effective alternative to antibody-based isolation kits, yielding MSC populations with comparable features and functions. The paper presents a robust and scalable methodology for investigating MSC-tumor interactions; hence, it enhances preclinical cancer research using murine models.

Materials and Methods

Animals and Cell Line Maintains

Swiss albino mice (6-8 weeks old, 20-25g body weight) were taken from the Institutional Animal Facility, AIIMS, New Delhi. All the mice were kept under standard hygienic laboratory conditions at a temperature of 25 ± 2°C, relative humidity (50–60%), light (12h light/12h dark cycle), providing the standard laboratory animal feed and water ad libitum. All experiments were conducted as per guidelines approved by the Institutional Animal Ethics Committee of the AIIMS, New Delhi, India (File no: 202/IAEC-1/2019). For the cell line, c127i cells were obtained from NCCS Pune and cultured in RPMI-1640 supplemented with 10% FBS, 1% penicillin-streptomycin antibiotic solution in CO2 incubator.

Reagents and Chemicals

α-MEM medium, fetal bovine serum (FBS) Gibco, Cat. No:26140079, penicillin-streptomycin, and trypsin-EDTA were purchased from Gibco by Life Technologies™. Tissue culture plate and culture flask were procured from Corning, USA. Antibodies like anti-CD44-FITC, anti-CD90-PE, anti-CD105-APC, anti-CD45-PerCP, and CD31-PE-Cy7 were purchased from Invitrogen, USA. All other chemicals were purchased from local firm and were of molecular grade with the highest purity.

Mice Dissection and Isolation of Bone Marrow-Derived MSCs

Healthy mice were taken and euthanized by cervical dislocation following established guidelines. After skin sterilization with 70% ethanol, tibias, femurs, and humeri were aseptically dissected. Soft tissues were carefully removed, and bones were transferred to sterile Petri dishes containing ice-cold complete α-MEM medium (supplemented with 15% FBS, 100 U/mL penicillin, and 100 µg/mL streptomycin).

Bones were washed twice with chilled PBS containing 1% penicillin-streptomycin. Bone marrow was flushed from medullary cavities using a 26-gauge needle in α-MEM medium plus 10% FBS. The flushed cells were collected in 15 mL conical tubes and centrifuged at 300 × g for 5 minutes. To maximize yield, the bones were subsequently cut into small fragments and crushed using a sterile mortar and pestle in chilled α-MEM medium plus 10% FBS.

The cell suspension (including bone fragments) was transferred to T-75 culture flasks and incubated at 37°C in a humidified atmosphere with 5% CO_2. After 48 hours, non-adherent cells were removed by replacing the medium. The

medium was changed every 3 days thereafter. Upon reaching 80-90% confluency (typically 7-10 days), cells were detached using 0.25% trypsin-EDTA and sub-cultured at a 1:3 ratio.

Morphological Characterization

Cellular morphology of BM-MSCs were monitored daily using an inverted phase-contrast microscope (Nikon Eclipse TS100). Images were captured at 4×, 10×, 20×, and 40× magnifications at days 1, 3, 5, 7, 14, and 21. Morphological parameters assessed included cell shape, size, confluence, and proliferation patterns.

Immunocytochemistry

Third-passage BM-MSCs grown on glass coverslips were fixed with 4% paraformaldehyde for 15 minutes at room temperature, permeabilized with 0.1% Triton X-100 for 10 minutes, and blocked with 3% bovine serum albumin for 1 hour. Cells were incubated overnight at 4°C with primary antibodies against CD44 (1:200) and CD90 (1:200), followed by appropriate fluorochrome-conjugated secondary antibodies (1:500) for 1 hour at room temperature. Nuclei were counterstained with DAPI (1 µg/mL). Images were acquired using a fluorescence microscope (Nikon Eclipse Ti2).

Flow Cytometric Analysis

BM-MSCs from passages 2-5 were analyzed for surface marker expression. Approximately 1×10^6 cells were suspended in staining buffer (PBS with 2% FBS) and incubated with fluorochrome-conjugated antibodies against CD44-FITC, CD90-PE, CD105-APC, CD45-PerCP, and CD31-PE-Cy7 for 30 minutes at 4°C in the dark. Isotype-matched antibodies served as controls. Cells were washed twice and analyzed using a BD FACSCanto II flow cytometer. Data were processed with FlowJo v10.0 software.

Preparation of Tumor-Conditioned Media

The mouse breast cancer cell line C127I was maintained in DMEM supplemented with 10% FBS and 1% penicillin-streptomycin. At 70-80% confluence, cells were washed twice with PBS and incubated with serum-free DMEM for 24 hours. The conditioned media was collected, centrifuged at 2000×g for 10 minutes to remove cellular debris, filtered through a 0.22 µm membrane, and stored at -80°C until use.

Induction of Tumor-Associated MSC Phenotype

BM-MSCs (passage 3-4) were seeded in 6-well plates at 1×10^5 cells/mL. After 24 hours, culture medium was replaced with either (1) complete α-MEM (control) or (2) 50:50 mixture of complete α-MEM and tumor-conditioned media (treatment). Cells were incubated for 48 hours before analysis.

Statistical Analysis

Data are expressed as mean ± standard error (SE) from at least three independent experiments. Statistical significance was determined using Student's t-test for comparisons between two groups or one-way ANOVA with Tukey's post-hoc test for multiple comparisons. A p-value < 0.05 was considered statistically significant. All analyses were performed using GraphPad Prism version 8.0.

Results

Passage-Dependent Adherent Purification of Morphological and Surface Markers Changes in Bone Marrow-Derived MSCs

The predominant feature of MSCs is extended cytoplasmic extension in the matures state of MSCs. The morphological progression of cultured mouse bone marrow-derived mesenchymal stem cells (BM-MSCs) was observed till 21 days in controlled conditioned (mentioned in material and method). The following characteristics features shown.

- Day 1, the culture predominantly comprised mononuclear cells interspersed with visible fat droplets.
- Day 3, spindle-shaped cells began to emerge among the mononuclear cells and fat droplets, marking the onset of differentiation.
- Day 5, the spindle-shaped cells reached approximately 60% confluence within the culture dish. Further proliferation and organization were evident by
- Day 7, when the spindle-shaped cells formed cohesive layers, prompting the first passage of the cells. By
- Day 9, where the culture reached up to 100% confluence, no further passage was required, indicating robust growth potential under the given conditions.
- Day 21, where the cells observed were from the third passage, MSCs showing extended cytoplasmic extension in the mature state of MSCs.

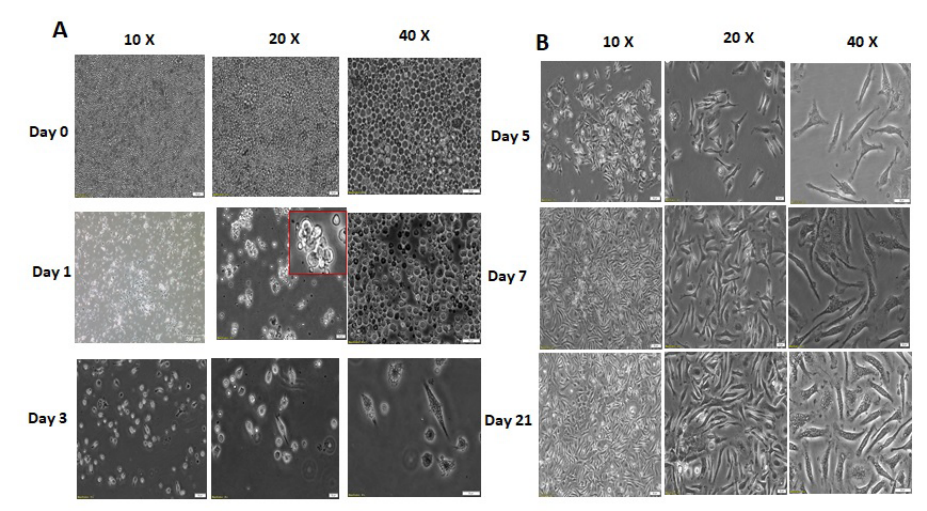

Figure 1a: Morphological Characteristics of BM-MSCs. (A) Spindle-shaped morphology of bone marrow–derived mixed cells observed by day 3 of culture. (B) A gradual increase in both the number and size of colonies from days 4 to 21. All images were captured at 40× magnification.

Fluorescent microscopy was performed to confirm the initial stage confirmation of MSC phenotype markers. CD44+ and CD90+ cell surface markers, with DAPI utilized for nucleus staining to visualize cell morphology. CD44-PE and CD90-FITC markers observed in the images reinforce the mesenchymal lineage of the cultured cells.

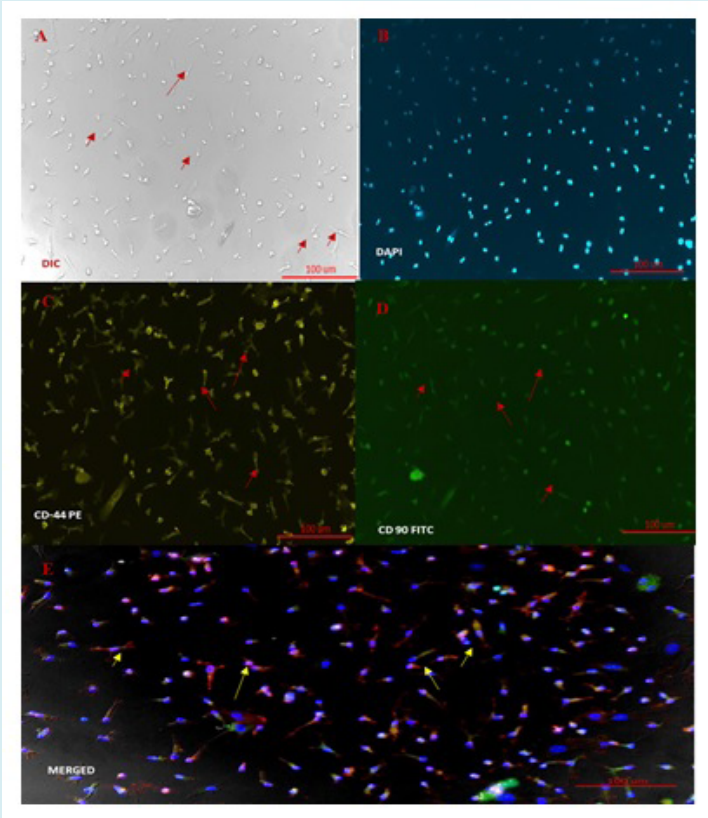

Figure 1b: Immunocytochemistry of MSCs. MSCs were positively stained with CD44 and CD90, with counterstaining using DAPI. All images were captured at 40× magnification.

Bone Marrow-Derived MSC Surface Marker Expression Indicates a Highly Homogeneous Cell Population

In order to confirm the surface marker, flow cytometry analysis was done of BM-MSCs at different passages, revealing a significant increase in the percentage of cells expressing the CD44 and CD105 markers associated with MSC identification. At Passage 3, nearly 92% of the cells were found to be negative for the endothelial marker CD31 and the leukocyte marker CD45, indicating a high purity of MSCs in the population. Moreover, these CD31 and CD45 negative cells showed strong positivity for CD44 and CD105, further confirming their mesenchymal stem cell identity (Figure 2a).

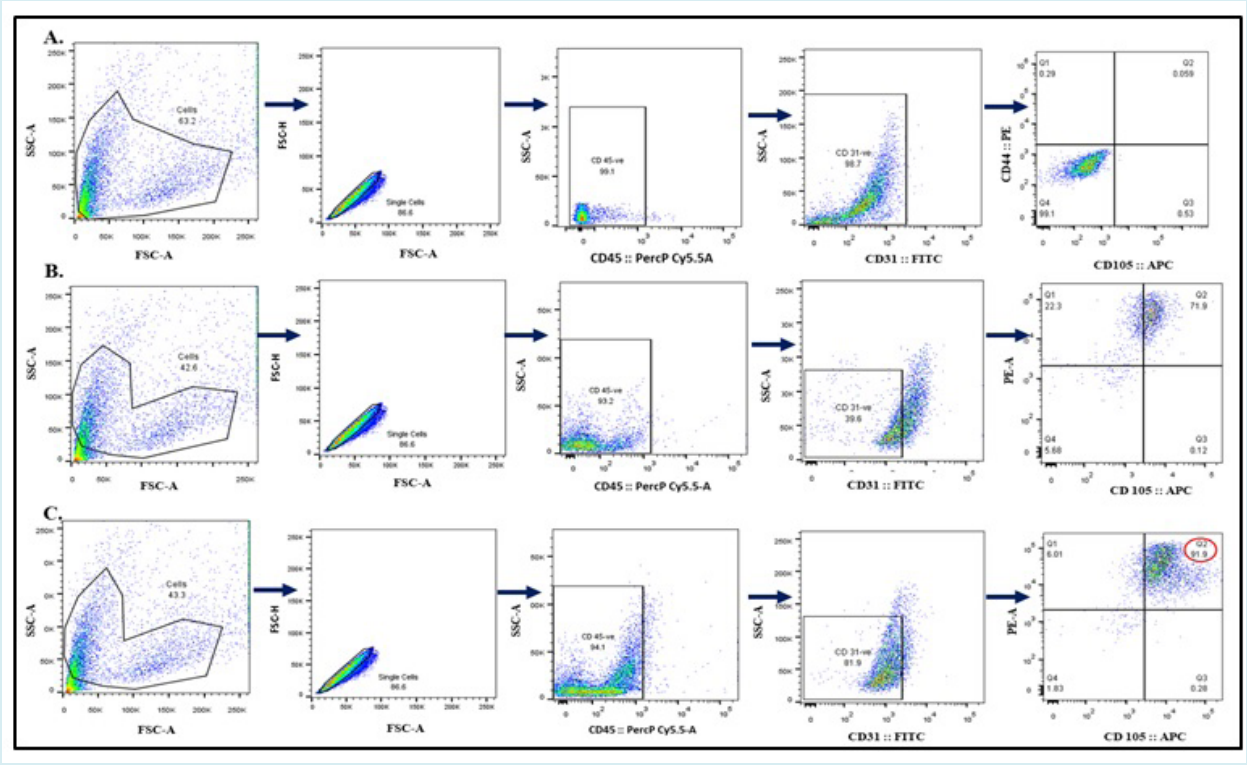

Figure 2a: Bone marrow-derived mesenchymal stem cells (BM-MSC) Surface markers expression by Flow Cytometry.

The flow cytometry analysis of BM-MSCs at various passages is depicted. (A) Gating strategy (B)At passage 2 the purity of MSCs were 71.9% (C) At Passage 3, nearly 92% of the cells were purily MSCs, CD31 negative cells were 94.1 & CD45 negative and were positive for CD44 and CD105, while the cells at Passage 2 and Passage 1 showed 71.9% and 0.059% positivity for these markers, respectively. These results indicate the successful isolation and enrichment of MSCs, thereby ensuring a highly homogeneous cell population.

In contrast, the percentages of CD44- and CD105-positive cells were low in Passage 2 and Passage 1 cells, with 71.9% and 0.059% positivity, respectively. This increasing trend in marker expression from Passage 1 to Passage 3 shows a steady growth of the MSC population over successive passages. These results show the successful isolation and characterization of BM-MSCs. They highlight the consistent improvement in the purity and homogeneity of the cell population with each passage. The standard deviations of these percentages would reflect the variability within the data sets. For example, in Passage 1, where the percentage of positively stained cells is 0.059%, a standard deviation value could indicate how dispersed the data points are around this mean percentage. Similarly, in Passage 2 with a positivity rate of 71.9%, a standard deviation value would provide insight into the variation among samples within that passage. However, without the specific dataset, the hypothetical standard deviation values cannot be accurately calculated (Figure 2b).

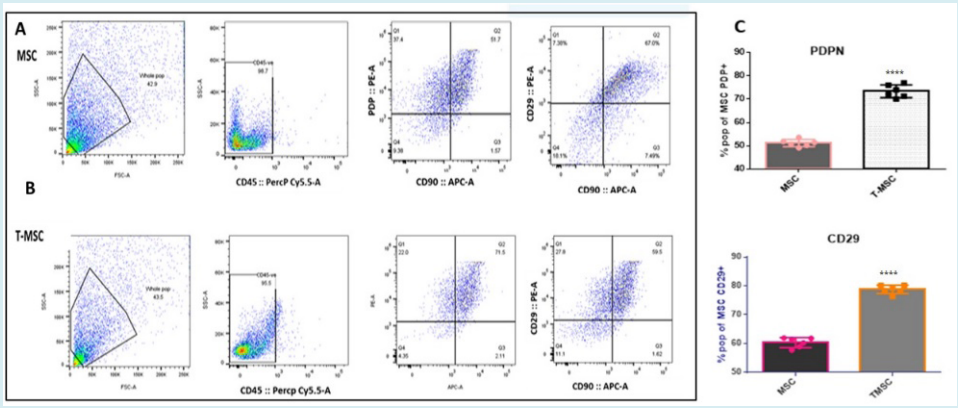

Figure 2b: Polarization of Bm-MSCs (Bone Marrow Mesenchymal Stem Cells) towards T-MSCs (Tumor-Associated Mesenchymal Stem Cells). Fig 2.5: (A) Pseudo plot of CD29 and Podoplanin in MSCs, with 59.5% and 51.7% expression, respectively. (B) Pseudo plot of CD29 and Podoplanin in TMSCs, with 67% and 71.5% expression, respectively. (C) Bar graph representation of the flow cytometry pseudo plot data, illustrating the increased expression of CD29 and Podoplanin in TMSCs compared to MSCs. . **p < 0.01, ***p < 0.001 and ****p < 0.0001, N= 6.

Polarization of Bm-MSCs) towards T-MSCs Confirmed using qPCR CD29, (C) Podoplanin, and (B) FSP

The microscopy analysis shows clear differences in the shapes of these cell types. The BM-MSCs (left image) have a distinctive spindle-shaped form typical of healthy mesenchymal stem cells. In contrast, the TMSCs (right image) have an altered appearance, marked by irregular outlines, more cell-to-cell interactions, and variations in size (Figure 3a). qPCR analysis of CD29, podoplanin, and fibroblast-specific protein (FSP) offered insights into the molecular changes linked to tumor conditioning. We observed different expression patterns between BM-MSCs and TMSCs, with a notable increase in podoplanin and FSP in TMSCs. Podoplanin, which is linked to tumor growth and spread, was particularly high in TMSCs, suggesting a potential role in enhancing tumor behavior. Likewise, the increased FSP expression in TMSCs points to a shift towards a stromal cell type, indicating their role in the tumor microenvironment (Figure 3b).

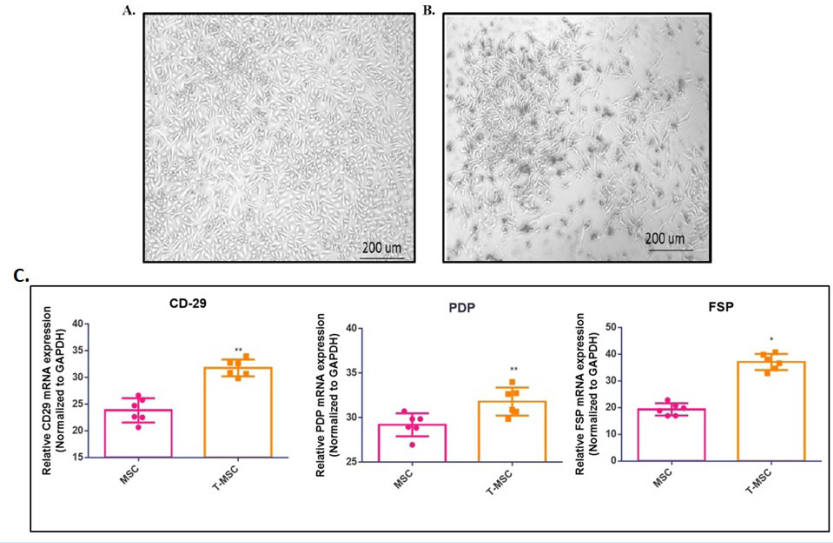

Figure 3: Phase-contrast microscopy was used to compare the shape of passage 3 bone marrow-derived mesenchymal stem cells (BM-MSCs) and tumor-conditioned mesenchymal stem cells (TMSCs). (A) BM-MSCs show a typical spindle shape that is common in healthy MSCs. (B) TMSCs have an altered shape, featuring irregular cell forms, increased interactions between cells, and variation in cell size. (C) The bar graph shows the relative gene expression levels, measured by real-time PCR, of key markers linked to MSC activation and tumor conditioning: (A) CD29, (B) FSP, and (C) Podoplanin. Data are presented as mean ± SEM (N = 6). Statistical significance is indicated as *p < 0.05 and **p < 0.01.

Discussion

In this study, we aimed to develop a cost-effective and reliable method for isolating, purifying, and characterizing BM-MSCs and their transformation into tumor-induced T-MSCs using tumor-conditioned media from Swiss albino mice. The immune system plays a crucial role in managing tumor growth and decline. Researchers have shown that MSCs not only help regulate the immune response in various conditions but also contribute to tumor growth and cancer progression. To effectively study MSCs, a pure population is necessary. While several methods exist for isolating MSCs, including immunomagnetic approaches, these can be expensive. Additionally, there are few standardized protocols for producing tumor-conditioned MSCs from Swiss albino mice. Therefore, we proceeded with the isolation, purification, and characterization of mouse bone marrow-derived MSCs and the induction of T-MSC phenotypes through tumor-conditioned media. We examined the morphology of the isolated BM-MSCs after seeding them in a flask. At first, the cells looked round and came in different sizes. On days three to five, they changed shape to look like a spindle. The cells were 60–70% confluent by day seven. Immunocytochemistry (ICC) tests on P-3 BM-MSCs showed that they had high levels of the surface markers CD44 and CD90, which confirmed that they were mesenchymal cells. Results from flow cytometry across different passages showed that MSCs were successfully isolated and improved. At P-3, about 92.0% (SD=2.3) of the cells were positive for CD44 and CD105. Microscopy analysis revealed the characteristic spindle morphology of healthy BM-MSCs, whereas T-MSCs displayed irregular shapes, enhanced cell-to-cell interactions, and size discrepancies, thereby validating the successful isolation and characterization of MSCs from mouse bone marrow. The results of flow cytometry showed that CD44 and CD105 expression in BM-MSCs slowly went up as the passages went on. At P- 3, 92.0% (SD=2.3) of the CD31- and CD45-negative cells exhibited these markers, in contrast to 71.9% (SD=2.4) at P-2 and merely 0.059% (SD=0.02) at P-1. These results confirm the successful isolation and enrichment of MSCs, leading to a homogeneous cell population. Our method of isolating cells, which combines flushing bones with mechanical disruption, gave us about 5–7×10^6 nucleated cells per mouse. By P 4, the MSC purity was over 95%. This level of efficiency is better than what has been found in other studies. The heightened MSC markers in subsequent passages correspond with the current literature; however, we observe that prolonged culture beyond P-5 may result in senescence or phenotypic alterations. Morphological assessment offers a straightforward yet efficient quality control measure. The change from mixed primary cultures to uniform spindle-shaped populations by passage 3 shows that MSCs have grown. This observation aligns with immunophenotypic data indicating maximum purity at P 3-4.

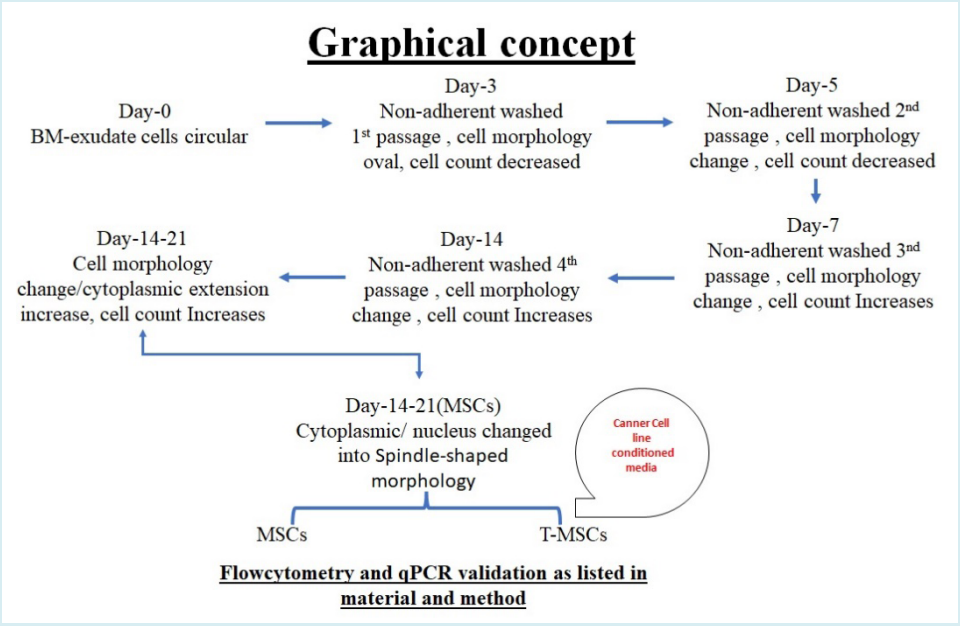

The application of conditioned media derived from C127I breast cancer cells effectively elicited tumor-like characteristics in MSCs. The changes in shape, like more irregularity and interactions between cells, are similar to what has been seen with carcinoma-associated fibroblasts, which suggests that the same pathways are being activated. The increased proliferation of tumor-conditioned MSCs substantiates the concept of a bidirectional MSC-tumor

signaling mechanism, wherein tumor-derived factors enhance stromal growth. There are a number of things to think about. First, Swiss albino mice serve as valuable models, yet strain-specific variations in MSC biology may be present. Second, using only one breast cancer cell line makes it harder to apply our results to other types of cancer. We need to test them on other types of cancer as well. Third, confirming the characteristics of tumor-conditioned MSCs in vivo would improve their applicability to physiological conditions. Our protocol has some good points, even though it has some flaws. For example, it only needs standard lab equipment, it is very reproducible across experiments, it includes thorough characterization through multiple techniques, and it can be changed for different cancer models by changing the source of conditioned media.

Conclusion

This protocol proposes a good way to look into how MSCs and tumors interact, test possible drugs, and make MSC-based delivery systems. An improved way to separate MSCs from Swiss albino mice that gives you MSCs with a high level of purity. Setting up a platform that can be used over and over again to look at how MSCs and tumors talk to each other and look for treatment options. In the future, researchers may look into how MSCs are drawn to tumors, how MSCs can make drugs less effective, and how to create cancer treatments that target MSCs.

Acknowledgment

The authors thank the Department of Biochemistry, AIIMS, New Delhi, for infrastructure support. We acknowledge the Central Instrumentation Facility (CIF) for access to tissue culture, fluorescence microscopy, flow cytometry, and real-time PCR facilities. Special thanks to the animal facility staff for technical assistance.

Funding

This work was supported by the Science and Engineering Research Board (SERB), Department of Science and Technology (DST), New Delhi (Grant No. EMR/2017/003209); the Indian Council of Medical Research (ICMR), New Delhi (Grant No. 5/13/8/2010/NCD-III); and the Intramural Research Grant (IRG), AIIMS, New Delhi (Grant No. A-IRC/2019/102).

Author Contributions

This work is part of PhD thesis work of Dr Anita Chauhan and she performed all the experiments and data analysis. PKG conceptualized the study, All authors reviewed and approved the final version of the manuscript.

Declaration

We have not used any AI tools or technologies to prepare this manuscript.

References

1. Pittenger MF, Mackay AM, Beck SC, Jaiswal RK, Douglas R, et al. (1999) Multilineage potential of adult human mesenchymal stem cells. Science 284(5411): 143-147.

2. Dominici M, Le Blanc K, Mueller I, Slaper-Cortenbach I, Marini F, et al. (2006) Minimal criteria for defining multipotent mesenchymal stromal cells. Cytotherapy 8(4): 315-317.

3. Friedenstein AJ, Chailakhyan RK, Latsinik NV, Panasyuk AF, Keiliss-Borok IV (1974) Stromal cells responsible for transferring the microenvironment of the hematopoietic tissues. Transplantation 17(4): 331-340.

4. Phinney DG, Prockop DJ (2007) Concise review: mesenchymal stem/multipotent stromal cells: the state of transdifferentiation and modes of tissue repair. Stem Cells 25(11): 2896-2902.

5. Barry FP, Murphy JM (2004) Mesenchymal stem cells: clinical applications and biological characterization. Int J Biochem Cell Biol 36(4): 568-584.

6. Caplan AI (1991) Mesenchymal stem cells. J Orthop Res 9(5): 641-650.

7. Mishra PJ, Mishra PJ, Humeniuk R, Medina DJ, Alexe G, et al. (2008) Carcinoma-associated fibroblast-like differentiation of human mesenchymal stem cells. Cancer Res 68(11): 4331-4339.

8. Galipeau J, Sensébé L (2018) Mesenchymal stromal cells: clinical challenges and therapeutic opportunities. Cell Stem Cell 22(6): 824-833.

9. Klopp AH, Gupta A, Spaeth E, Andreeff M, Marini F (2011) Concise review: dissecting a discrepancy in the literature: do mesenchymal stem cells support or suppress tumor growth? Stem Cells 29(1): 11-19.

10. Spaeth EL, Dembinski JL, Sasser AK, Watson K, Klopp A, et al. (2009) Mesenchymal stem cell transition to tumor-associated fibroblasts contributes to fibrovascular network expansion and tumor progression. PLoS One 4(4): e4992.

11. Quante M, Tu SP, Tomita H, Gonda T, Wang SSW, et al. (2011) Bone marrow-derived myofibroblasts contribute to the mesenchymal stem cell niche and promote tumor

growth. Cancer Cell 19(2): 257-272.

12. Ridge SM, Sullivan FJ, Glynn SA (2017) Mesenchymal stem cells: key players in cancer progression. Mol Cancer 16(1): 31.

13. Karnoub AE, Dash AB, Vo AP, Sullivan A, Brooks MW, et al. (2007) Mesenchymal stem cells within tumour stroma promote breast cancer metastasis. Nature 449(7162): 557-563.

14. Ren G, Zhao X, Wang Y, Zhang X, Chen X, et al. (2012) CCR2-dependent recruitment of macrophages by tumor-educated mesenchymal stromal cells promotes tumor development and is mimicked by TNFα. Cell Stem Cell 11(6): 812-824.

15. Lamouille S, Xu J, Derynck R (2014) Molecular mechanisms of epithelial-mesenchymal transition. Nat Rev Mol Cell Biol 15(3): 178-196.

16. Kalluri R (2016) The biology and function of fibroblasts in cancer. Nat Rev Cancer 16(9): 582-598.

17. Cuiffo BG, Karnoub AE (2012) Mesenchymal stem cells in tumor development: emerging roles and concepts. Cell Adh Migr 6(3): 220-230.